

TABLE II. Energy, E_0 , in units of $\rho\kappa^2r_0$, of a circular vortex ring of strength κ with an empty streamlined core in an unbounded fluid, for various ratios of the ring radius r_0 to the core radius a .

r_0/a	$E_0/\rho\kappa^2r_0$	r_0/a	$E_0/\rho\kappa^2r_0$	r_0/a	$E_0/\rho\kappa^2r_0$
10	1.109	100	2.328	1 000	3.492
20	1.487	200	2.681	2 000	3.840
30	1.703	300	2.887	3 000	4.043
40	1.855	400	3.032	4 000	4.187
50	1.971	500	3.144	5 000	4.298
60	2.066	600	3.236	6 000	4.389
70	2.145	700	3.313	7 000	4.466
80	2.214	800	3.381	8 000	4.533
90	2.274	900	3.440	9 000	4.592
				10 000	4.645
				>10 000	$\frac{1}{2} \ln(8r_0/a) - 1$

where the exponential integral Ei is a tabulated function¹⁵ defined by $-Ei(-x) \equiv \int_x^\infty t^{-1}e^{-t}dt$. Values of $E_0/\rho r_0 \kappa^2$, which are given in Table II, were computed

on a desk calculator using Eq. (20) with $N=20$. They are accurate to within 0.1%.

The difference between these values and those given by Eq. (13) is indeed small for reasonable a , being less than 1% if $r_0/a > 100$, and less than 0.1% if $r_0/a > 500$. As is to be expected, the results are also very close to those of Eq. (11) if a/r_0 and r_0/R are both very small. Hence, as is shown in Fig. 6, the ratio of the energy of an enclosed ring to that of an unenclosed ring with the same r_0 and a goes to unity as r_0 becomes small, as long as r_0 does not become comparable with a . If this last condition is not satisfied, the energy of the enclosed ring actually becomes a little higher than that of the unenclosed ring, owing to distortion of the core. The effect is about 1∞ for $10a=r_0=0.1R$. It is clearly irrelevant to the present application of this calculation.

Energy Distribution of Electrons Ejected from Tungsten by He⁺ †

F. M. PROPST

Department of Physics, University of Illinois, Urbana, Illinois

(Received 16 July 1962; revised manuscript received 3 October 1962)

The results of a calculation of the energy distribution of electrons ejected from tungsten by low-energy He⁺ are presented. The calculation is based on a mechanistic model of the process in which the ejected electrons are divided into two groups: (1) the electrons excited in the primary process that can escape directly; and (2) the electrons that escape because of interactions between the primary electrons and those of the band structure of the solid. Secondary electron data are used to predict the portion due to this second mechanism.

I. INTRODUCTION

THE potential ejection of electrons from solid surfaces by low-energy ions has been studied extensively both experimentally and theoretically.¹⁻⁶ Since the phenomenon is sensitive to the surface structure, both the experimental and theoretical treatments are quite complicated. In this paper we give the preliminary results of a calculation (based on a mechanistic model of the process) of the energy distribution of electrons ejected from tungsten by He⁺. We attempt to take into account the interactions of the electrons excited in the

primary Auger process with those of the band structure of the solid. In the case under discussion, these interactions appear to give rise to about 50% of the total measured yield.

In order to calculate the energy distribution of electrons ejected by ions, we must know: (1) the distribution in energy and angle, $N(E, \Omega)$, of the electrons excited inside the metal in the primary process; (2) the escape probability, $F(E, \Omega)$, of the electrons; and (3) the effect of interactions between the primary electrons and the electrons of the solid. These items are treated in the following sections.

II. ENERGY DISTRIBUTION OF PRIMARY ELECTRONS

Figure 1 shows a sketch commonly used to describe the situation that exists when an ion approaches a solid surface. One electron falls into the vacant atomic level. The energy released in the transition is then absorbed by a second electron from the solid. We can look at the process in two ways. First, we can assume that the Coulomb interaction between the two participating

† The research reported in this paper was made possible by support extended to the University of Illinois, Coordinated Science Laboratory, jointly by the Department of the Army (Signal Corps and Ordnance Corps), Department of the Navy (Office of Naval Research), and the Department of the Air Force (Office of Scientific Research, Air Research and Development Command) under Signal Corps Contract DA-36-039-SC-85122.

¹ H. S. Massey, Proc. Cambridge Phil. Soc. **26**, 386 (1930).

² S. S. Shekhter, J. Exptl. Theoret. Phys. (USSR) **7**, 750 (1937).

³ A. Cobas and W. E. Lamb, Jr., Phys. Rev. **65**, 327 (1944).

⁴ H. D. Hagstrum, Phys. Rev. **96**, 336 (1954).

⁵ H. D. Hagstrum, Phys. Rev. **119**, 940 (1960).

⁶ D. Sternberg, Ph.D. thesis, Columbia University (unpublished).

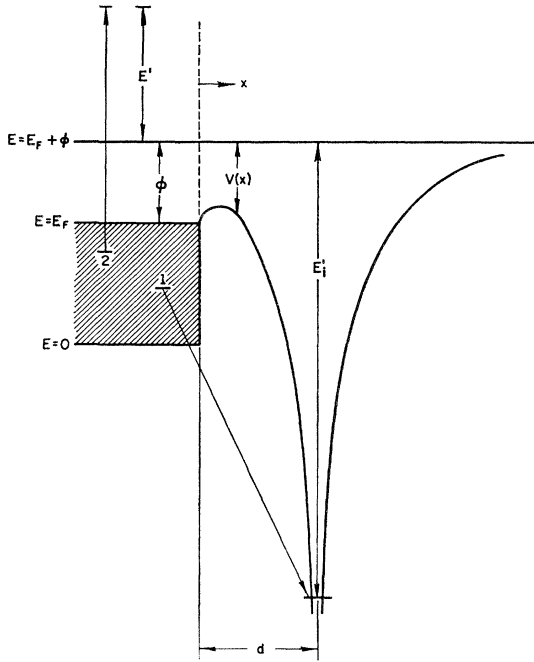


Fig. 1. Energy level diagram of the ion-metal surface system, illustrating Auger neutralization of the ion.

electrons is the perturbation that causes the transition. Alternatively, we can take the radiation field set up by the first electron when it falls into the atomic level as the perturbation that excites the second electron. Burhop⁷ has shown that in the nonrelativistic limit the two approaches give the same results. If we look at the process from this second point of view, we can divide the problem into two parts. First, we must calculate the probability that the first electron "radiates" and then the probability that a second electron absorbs the radiation.

In the dipole radiation matrix element

$$e \int \psi_{at} \nabla \psi_{ml} d\tau, \quad (1)$$

the atomic ground-state wave function, ψ_{at} , is strongly localized around the ion. The integral is then approximately of the form,

$$k \psi_{ml}(0), \quad (1)$$

where $\psi_{ml}(0)$ is the value at the ion core of the wave function of the electron initially in the metallic state ml. Thus, the probability, w , that an electron initially in this state falls into the atomic level is

$$w = A |\psi_{ml}(0)|^2. \quad (3)$$

As an estimate of the relative value of $|\psi_{ml}(0)|^2$, we use the WKB transmission probability

$$|\psi_{ml}(0)|^2 \propto h(E_x, V) \times \exp \left[-2 \left(\frac{2m}{\hbar^2} \right)^{1/2} \int_0^{x_m(E_x)} [E_x - V(x)]^{1/2} dx \right], \quad (4)$$

where $x_m(E_x)$ is the turning point at the ion side of the barrier, $V(x)$ is the potential along the normal between the ion and the metal surface, E_x is the kinetic energy corresponding to the component of the k vector normal to the surface, and $h(E_x, V)$ is a slowly varying function which we shall take to be unity. Assuming that the potential $V(x)$ is given by the Coulomb potentials of the ion, the image of the ion, and the image of the electron, we have

$$V(x) = -3.6 \left(\frac{1}{x+x_c} + \frac{8x}{d^2-x^2} \right), \quad (5)$$

where V is in eV, x is the coordinate normal to the surface measured in angstroms, x_c is chosen to make the potential equal to minus the work function at x equal to zero, and d is the ion-surface separation.

By numerical integration, we have found, to a good degree of approximation, that

$$2 \left(\frac{2m}{\hbar^2} \right)^{1/2} \int_0^{x_m(E_x)} (E_x - V)^{1/2} dx = a(d)(E_F - E_x) + b(d), \quad (6)$$

where E_F is the Fermi energy and $a(d)$ was found to vary as shown in Fig. 2. Since we are interested in the variation of the transition probability with the total initial energy of the electron, we must integrate (6), weighted by the appropriate state density function, over E_x at constant E . However, this merely introduces a slowly varying function of E which, like $h(E_x, V)$, we shall neglect in this first treatment. Thus, the probability that an electron with initial kinetic energy E takes part in a transition to the atomic level when the ion is at a distance d is

$$w(d, E) = B(d) \exp[-a(d)(E_F - E)]. \quad (7)$$

The energy, E_ω , released in such a transition is

$$E_\omega = E_i'(d) - \phi - (E_F - E), \quad (8)$$

where $E_i'(d)$ is the effective ionization potential of the ion and ϕ is the work function of the metal. Thus, in terms of the energy released, we have

$$w(d, E_\omega) = B(d) \exp\{-a(d)[E_i'(d) - \phi - E_\omega]\}.$$

For the second stage of the excitation process, we assume that: (1) The density of states of the conduction band is constant⁸; (2) the temperature of the system is 0°K; (3) the probability of absorption is independent of the initial state of the absorbing electron and of the

⁷ E. H. S. Burhop, *The Auger Effect and Other Radiationless Transitions* (Cambridge University Press, New York, 1952).

⁸ The calculations of M. F. Manning and M. I. Chodorow [Phys. Rev. **56**, 787 (1939)] show that this is a good approximation.

energy, E_ω , absorbed; and (4) the majority of the transitions take place when the ion is within a small range of a critical distance, d_0 , from the surface.⁴

Using these assumptions, we find that the energy distribution inside the metal, $N_i(E)$, of the electrons excited in the Auger process is

$$\begin{aligned} N_i(E) &= B \int_{-\eta}^{\eta} \exp[-a(E_F - \eta - x)] dx, \\ &\quad R \leq E \leq R + E_F, \\ &= B \int_{-(E_F - \eta)}^{(E_F - \eta)} \exp[-a(E_F - \eta - x)] dx, \\ &\quad R + E_F \leq E \leq R + 2E_F, \end{aligned} \quad (10)$$

where $a = a(d_0)$ and $\eta = (E - R)/2$ and R is the minimum energy of the excited electrons,

$$R = E_i' - E_F - \varphi. \quad (11)$$

Integrating and normalizing to one electron excited per incident ion i.e., assuming all ions are neutralized by this process, we get

$$\begin{aligned} N_i(E) &= \frac{\exp\{-a[E_i'(d) - \varphi - E]\} - \exp(-aE_F)}{E_F[1 - \exp(-aE_F)]}, \\ &\quad E_i' - \varphi - E_F \leq E \leq E_i' - \varphi \\ &= \frac{1 - \exp\{-a[E_i'(d) + E_F - \varphi - E]\}}{E_F[1 - \exp(-aE_F)]}, \\ &\quad E_i' - \varphi \leq E \leq E_i' + E_F - \varphi. \end{aligned} \quad (12)$$

Figure 3 shows $N_i(E)$ for a equal to 0.3, 0.4, and 0.5 eV^{-1} . This corresponds, according to Fig. 2, to d equal to 2.05, 2.35, and 2.66 \AA , respectively. Hagstrum⁴ has derived the effective ionization potential, $E_i'(d)$, for He^+ . His results are shown in Fig. 2. From this curve, we find the effective ionization potentials for the three

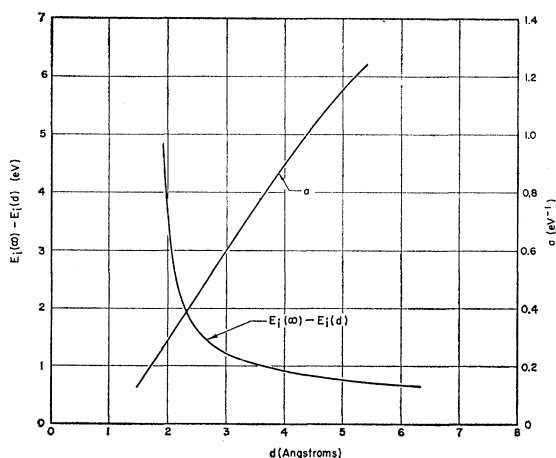


FIG. 2. Plots of the variation of the effective ionization potential (reference 4) and of the exponential factor, a , with the ion-surface separation.

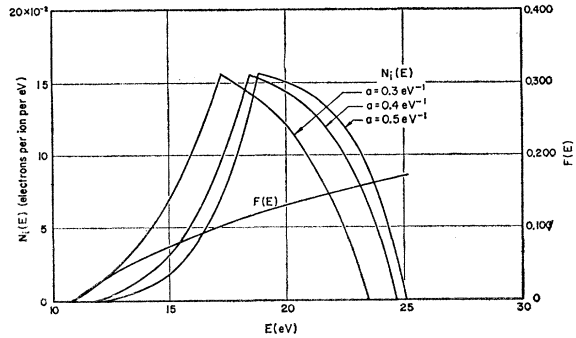


FIG. 3. Plots of the internal energy distribution, $N_i(E)$, [Eq. (12)], and of the escape factor, $F(E)$, [Eq. (15)]. The effective ionization potentials as determined from Fig. 2 were used in plotting the $N_i(E)$ curves.

values of a above, to be 21.6, 22.8, and 23.2 eV, respectively. These values have been used in plotting Fig. 3.

In this paper, we take the angular distribution of the excited electrons to be isotropic for all energies. While this is obviously not the most likely distribution, its simplicity is appealing. We have done the same calculation using an angular distribution with the shape of a prolate spheroid, the major axis being normal to the surface and the ratio of the major to minor axes being 4/3. The results obtained using this distribution are in better agreement with the experimental curve. We shall not present these results here since the simpler form, i.e., the isotropic distribution, is more in keeping with the approximations and assumptions used in the rest of the calculation.

III. PROBABILITY OF ESCAPE

Having an energy-angular distribution, we must next consider the problem of how the electrons escape from the metal. The electrons that escape can be divided into two classes. A fraction of those excited in the primary process have a large enough component of momentum directed towards the surface that they are able to escape from the metal. However, there is a large fraction of the primary electrons that do not satisfy this condition and cannot pass over the surface barrier directly. There is the possibility that these electrons can then interact with the other electrons of the solid, producing electrons that can escape. This latter possibility will be considered in the next section.

We shall consider that all electrons escape from the metal that have a component of momentum, p_n , normal to the surface such that

$$p_n^2/2m \geq E_b, \quad (13)$$

where $E_b = E_F + \varphi$ is the surface barrier. This condition on p_n defines a cone, the axis of which is normal to the surface, with a half-angle θ_c , where

$$\theta_c = \cos^{-1}[(E_b/E)^{1/2}]. \quad (14)$$

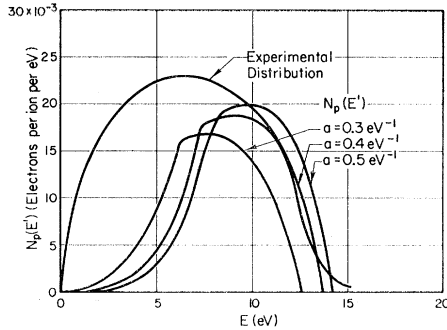


FIG. 4. Comparison of $N_p(E')$, (Eq. 16), with the experimental distribution (reference 9).

The total momentum vectors of the electrons that can escape lie within this cone. Thus, for an isotropic angular distribution, the fraction, F , of electrons with energy E that escape is given by

$$F(E) = \frac{1}{2} [1 - (E_b/E)^{1/2}]. \quad (15)$$

The "primary" energy distribution, $N_p(E')$, is then

$$N_p(E') = F(E' + E_F + \varphi) N_i(E' + E_F + \varphi), \quad (16)$$

where E' is the external kinetic energy of the escaping electron.

In Fig. 4, we show the $N_p(E')$ curves for the three values of a listed previously. We also show an experimentally determined distribution⁹ for 100-eV He⁺ incident on tungsten. It is interesting to note that the curve for $a=0.4$ ($d_0=2.35$ Å, $E_i'=22.8$ eV) gives a good fit to the high-energy edge of the experimental distribution in two ways. First, it "fits" this portion of the curve. Second, its position on the energy scale, which is determined by the effective ionization potential, is such that it coincides with the experimental curve. The fact that these two independent criteria are satisfied gives us some confidence in the assumptions used in the calculation. It is also interesting to note that the value of d_0 (2.35 Å) determined here agrees well with the value of 2.2 Å estimated by Hagstrum.⁴

We must note at this point that there are two effects neglected in this treatment that tend to cancel one another. First, as mentioned earlier, the angular distribution is probably peaked in the direction normal to the surface. This would increase the magnitude of $N_p(E')$. Second, some of the electrons that have sufficient momentum normal to the surface to escape would be scattered, thus reducing the $N_p(E')$ distribution. A firmer calculation of the shape of the angular distribution is needed to shed light on the relative importance of these two effects.

IV. THE EFFECT OF ELECTRON-ELECTRON INTERACTIONS

The energy distribution, $N_i'(E)$, of the primary Auger electrons that cannot escape directly from the

⁹ H. D. Hagstrum, J. Appl. Phys. 31, 715 (1960); Phys. Rev. 96, 3251 (1954).

metal is

$$N_i'(E) = [1 - F(E)] N_i(E). \quad (17)$$

We assume the secondaries caused by these electrons to have the same energy distribution as the secondaries caused by external electrons introduced into the metal with the energy profile $N_i'(E)$.

Harrower¹⁰ has measured the relative energy distributions of secondary electrons from polycrystalline tungsten produced by 7-, 10-, and 20-eV primary electrons. Morgulis and Gorodetskii¹¹ have determined the total yield and "pure" secondary yield for low-energy electrons incident on polycrystalline tungsten. These results were combined to obtain the absolute energy distributions for the three primary energies listed. The $N_i'(E)$ distribution was then divided into three regions, corresponding approximately to the three values of primary energy available. The secondary distributions, omitting the portion due to reflected electrons, were then weighted by the fraction of electrons in the respective regions. The results are shown in Fig. 5. The sum, $N_s(E')$, of the three resulting curves gives approximately the "secondary" portion of the energy distribution of the Auger electrons. This curve has been normalized so that the area under it is equal to

$$\int [1 - F(E' + E_F + \Phi)] \times N_i(E' + E_F + \Phi) \frac{\Delta(E')}{1 - r(E')} dE', \quad (18)$$

where $\Delta(E')$ is the "pure" secondary yield and $r(E')$ is the reflection coefficient given in reference 11. We

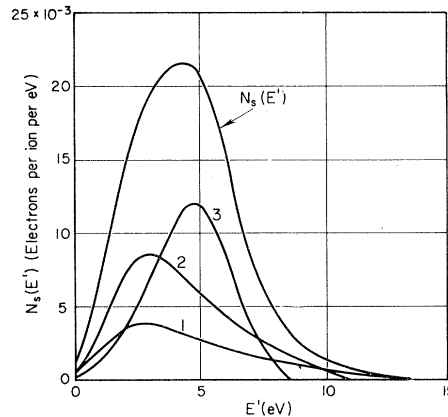


FIG. 5. Construction of the energy distribution, $N_s(E')$, of secondaries caused by electron-electron interactions. Curves 1, 2, and 3 are the distributions arising from the portions of $N_i'(E')$ centered at 13, 10, and 7 eV, respectively. Curve 1 was approximated from the results Harrower (reference 10) obtained for 20-eV primary energy (there were no data available for 13 eV).

¹⁰ G. A. Harrower, Phys. Rev. 104, 52 (1956).

¹¹ N. D. Morgulis and D. A. Gorodetskii, Soviet Phys.—JETP 3, 535 (1956).

have used $\Delta/(1-r)$ since we want the secondary yield of the electrons that actually penetrate the metal.

Figure 6 shows the total energy distribution predicted by this treatment along with the experimental curve.⁹ We have shown the results obtained using the $N_s(E')$ distribution of Fig. 5. We have also shown the results using $N_s(E')$ derived in the same manner described above but using the data obtained by Gorodetskii¹² for the secondary emission from single crystal tungsten. The experimental distribution shown is that for 100-eV He^+ on polycrystalline tungsten.⁹

We must note at this point that the secondary data used are for electrons normally incident on the surface, while the Auger electrons are distributed over all angles. Although the data available for the yield as a function of the angle of incidence tend to show that there is no angular dependence at low energies, it is not clear that this should be the case at these very low energies. Here there are only a small number of collisions between the primary and the conduction electrons. Hence, we might expect the initial direction of the primary to influence the number of secondaries that can be produced. We also note that if the depth of penetration of the external electrons is not of the same order as the excitation depth of the Auger electrons, we would not be able to use the secondary data to fit the Auger distribution.

The total Auger yield given by this treatment is 12.4%, due to the Auger electrons that can escape directly and 12.0% due to the electron-electron interactions (based on the secondary data for polycrystalline tungsten¹¹). The total measured yield is 24.0% for 100-eV He^+ .

V. SUMMARY

We have given the results of a simplified treatment of the ejection of electrons from tungsten by He^+ . The agreement between the experimental distribution and the one predicted by this method is reasonably good. Specifically, we feel that the agreement is sufficiently good to give substance to the hypothesized importance of the electron-electron interactions. It is possible that this treatment or some modification of it might also be

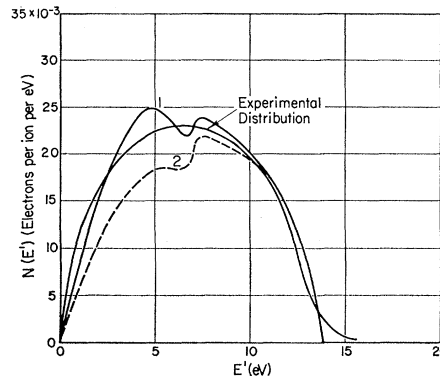


FIG. 6. Comparison of the theoretical and experimental distributions. Curve 1 is obtained using $N_s(E')$ shown in Fig. 5. Curve 2 is obtained using $N_s(E')$ derived from secondary emission data for single-crystal tungsten.

applicable to other systems. In particular, the technique of using secondary electron data to fit the low-energy portion of the distribution might be applied to the energy distributions of photoelectrons.¹³

The complete treatment, starting from first principles, of this problem is quite complex. The calculation given in this paper involves simplifying assumptions in order to take into account two factors that have been left out of previous treatments. That is, the perturbation of the wave function of the metallic electron by the Coulomb potential of the ion (through the use of the WKB approximation) and the effect of electron-electron interactions. However, the simple nature of the assumptions made does lead us to believe that there is some chance involved in the close agreement between the predicted and measured total yields. It is hoped that the application of this treatment to other systems will shed more light on the importance of the various processes.

ACKNOWLEDGMENTS

It is a pleasure to thank Dr. Hans Frauenfelder for critical reading of the manuscript. The author is particularly grateful to his advisor, Dr. Edgar Lüscher and to Dr. D. G. Ravenhall for many helpful discussions during the preparation of this paper.

¹² D. A. Gorodetskii, Soviet Phys.—JETP 7, 4 (1958).

¹³ J. Dickey, Phys. Rev. 81, 612 (1951).